

Interaction induced local moments in parallel quantum dots within the functional renormalization group approach

V. S. Protsenko and A. A. Katanin

*M. N. Mikheev Institute of Metal Physics, 620990 Ekaterinburg Russia
Ural Federal University, 620002 Ekaterinburg, Russia*

(Dated: December 9, 2024)

We propose a version of functional renormalization-group (fRG) approach, which is, due to including Litim-type cutoff and switching off (or reducing) the magnetic field during fRG flow, capable describing singular Fermi liquid (SFL) phase, formed due to presence of local moments in quantum dot structures. The proposed scheme allows to describe the first-order quantum phase transition from "singular" to the "regular" paramagnetic phase with applied gate voltage and shows sizable spin splitting of electronic states in the SFL phase in the limit of vanishing magnetic field $H \rightarrow 0$. The calculated conductance shows good agreement with the results of the numerical renormalization group.

Introduction. During last decades electronic and transport properties of quantum dots have attracted considerable attention due to possibility of realizing non-trivial quantum phenomena and promising applications in different nanodevices [1, 2], in particular quantum computation systems [3–8]. The electron-electron interaction may have significant effect on electronic properties and transport in quantum dot systems and is responsible for many interesting physical phenomena.

While relatively strong Coulomb interaction leads to Kondo effect [9–12], for some special geometries of quantum dot systems even relatively weak interaction plays important role. This concerns in particular a system of parallel quantum dots, connected symmetrically to common leads, where the formation of the so called singular Fermi liquid (SFL) state [13, 14], which possesses a local moment, decoupled from the leads, and almost unitary conductance, is possible near half filling.

To date, a wide variety of analytical and numerical methods have been developed to describe the effect of the Coulomb interaction in quantum dot structures. The numerical renormalization group (NRG) method provides a straightforward approach to describe spectral functions and conductivity of quantum dots in the presence of an interaction [15–18]. However, being very successful, this method requires significant computational effort, which grows exponentially with the number of interacting degrees of freedom. This circumstance does not allow one to directly apply these methods to fairly large systems.

The recently proposed nanoscopic dynamic vertex approximation (nano-DFA) [19, 20], allows one to treat effects of interaction in nanostructures, and has a potential of describing non-local correlations beyond nano-DMFT [21–25]. In the most complete, parquete, formulation nano-DFA approach however also requires substantial computational resources.

In this regard, the recently proposed functional renormalization-group (fRG) approach [26–28] is very promising because it allows to reformulate a many particle problem in terms of coupled differential equations for irreducible vertex functions, which, after several approximations, can be easily integrated even for complex

systems. This method has already been successfully applied to systems consisting of a small number of quantum dots arranged in different geometries [29–32]. In these studies it was shown that the results obtained with the sharp frequency cutoff are in good agreement with the Bethe ansatz and NRG data [30]. At the same time, the fRG approach with the sharp cutoff scheme is not applicable to describe the SFL state, since, e.g., for parallel quantum dots it yields an artificially low conductance at low magnetic fields for gate voltages V_g less than some critical value $|V_g| \lesssim V_g^c$ [30], which contradicts the NRG results [13].

To describe physical properties in the local moment SFL state, we propose in the present paper an fRG scheme with continuously switching off (or decreasing) the external magnetic field with decreasing cutoff. This scheme is similar to a counterterm technique, used earlier to treat the first order quantum phase transitions in lattice fermionic systems [33, 34] within fRG approach. This technique was not however applied to description of quantum dot structures. We show that within this approach it is possible to describe correctly the dependence of the conductance on the magnetic field and the gate voltage in a good agreement with NRG data.

Model. The parallel quantum dots symmetrically connected to two conducting leads can be modelled by the Hamiltonian $\mathcal{H} = \mathcal{H}_{\text{dot}} + \mathcal{H}_{\text{leads}} + \mathcal{H}_{\text{coup}}$, where

$$\mathcal{H}_{\text{dot}} = \sum_{j\sigma} \left[\epsilon_{\sigma}^0 n_{j,\sigma} + \frac{U}{2} \left(n_{j,\sigma} - \frac{1}{2} \right) \left(n_{j,\bar{\sigma}} - \frac{1}{2} \right) \right] \quad (1)$$

describes quantum dots with equal on-site Coulomb repulsion U and single energy level $\epsilon_{\sigma}^0 = V_g - \sigma H/2$, controlled by the gate voltage V_g and magnetic field H , $d_{j,\sigma}^{\dagger}$ ($d_{j,\sigma}$) – denote creation (annihilation) operators for an electron with spin σ localized on the j -th quantum dot and $n_{j,\sigma} = d_{j,\sigma}^{\dagger} d_{j,\sigma}$, $\mathcal{H}_{\text{leads}}$ takes into account the two equivalent non-interacting semi-infinite leads, and the last term $\mathcal{H}_{\text{coup}}$ introduces symmetric coupling between each quantum dot and leads [35].

Method. To describe the correlation effects in quantum dots, we, following to Ref. [30], project out the leads,

introduce some cutoff of the bare single-particle Green function of the dots $\mathcal{G}_0 \rightarrow \mathcal{G}_0^\Lambda$, and apply the one-particle irreducible fRG scheme [27, 28], yielding an infinite hierarchy of differential flow equations for the self-energy Σ and the n -particle vertices $\Gamma^{(2n)}$, $n \geq 2$. Truncating the fRG flow equations by neglecting of the flow of the vertex functions with $n \geq 3$ leads to a closed system of the flow equations for the Σ and the two-particle vertex $\Gamma^{(4)}$, which has the standard form [29, 30, 35]. As in Refs. [29, 30] we neglect frequency dependence of the self-energy and two-particle vertices.

The standard fRG scheme to study a correlated quantum dots uses sharp cutoff in frequency space [29–32] $\mathcal{G}_0 \rightarrow \Theta(|\omega| - \Lambda)\mathcal{G}_0$, where Heaviside theta function Θ cuts out infrared modes with Matsubara frequency $|\omega| < \Lambda$. Fig. 1 shows that there is a clear qualitative difference between the magnetic field H dependence of the conductance $G(H)$ at the half-filling ($V_g = 0$) within the NRG approach, applied following Refs. [36–38], and the fRG approach based on the sharp cutoff scheme [35]. The conductance obtained within the latter approach first smoothly increases with decreasing magnetic field and then suddenly drops when the magnetic field becomes sufficiently small, in contrast to the NRG result. This drop of the conductance originates from the unphysical behavior of the vertex functions in the fRG flow, namely, with decreasing of the magnetic field they first converge to finite, but unphysically large values, and, for even smaller fields, diverge at $\Lambda \rightarrow 0$.

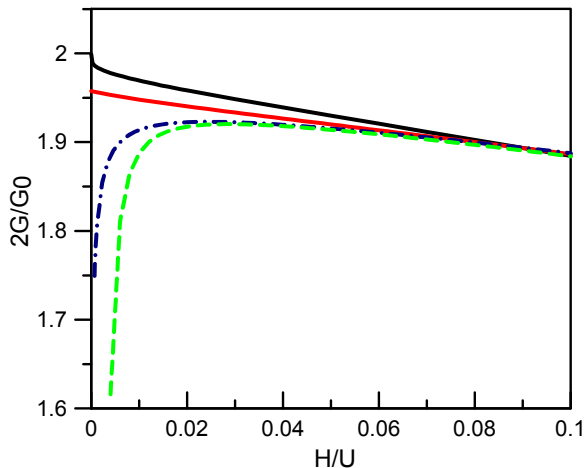


FIG. 1. (Color online). Linear conductance $2G/G_0$ ($G_0 = 2e^2/h$) as a function of magnetic field H for $U = 2\Gamma$ and $V_g = 0$. Dashed green and dashed-dotted blue lines correspond to fRG approximation in the sharp-cutoff and Litim-type cutoff scheme, respectively. Solid black upper line: NRG calculation. Solid red line: fRG approach with the counterterm χ_1^Λ with $\tilde{H} = 0.1$ and $\Lambda_c = 0.05$.

The results of the approach with sharp cutoff can be somewhat improved using Litim-type [39] Λ -dependence of the bare propagator [40]

$$\left[\tilde{\mathcal{G}}_{0,\sigma}^\Lambda\right]^{-1} = \left[\mathcal{G}_{0,\sigma}\right]^{-1} + iI(\Lambda - |\omega|)\Theta(\Lambda - |\omega|)\text{sign}(\omega),$$

where I is the 2×2 identity matrix. Using this cutoff, we find that over the whole range of studied magnetic fields the conductance is larger than that obtained in the fRG approach with the sharp momentum cutoff (see Fig. 1), which leads to some improvement of agreement with NRG data for not too low magnetic fields and allows us to continue the renormalization group flow toward a weaker magnetic fields.

Despite some improvement of the results, the smooth cutoff itself does not allow to describe correctly conductivity at small magnetic fields. Furthermore, we found that at low magnetic field these fRG schemes break down not only for the half-filling ($V_g = 0$), as considered above, but also when $|V_g| < V_g^c$, where V_g^c is a critical value of gate voltage, which is discussed below. We consider this situation as rather general, and related to the formation of the SFL state in zero magnetic field, that according to the phase diagram obtained in Ref. [14] occurs near half filling.

To describe the SFL state we decrease the magnetic field continuously during the flow, similarly to a counterterm extension of the fRG [33, 34]. To this end, we introduce additional term $\sigma\chi^\Lambda/2$ in the propagator of the quantum dots

$$\mathcal{G}_{0,\sigma}^\Lambda = \left\{ \left[\tilde{\mathcal{G}}_{0,\sigma}^\Lambda\right]^{-1} + \frac{\sigma}{2}I\chi^\Lambda \right\}^{-1}, \quad (2)$$

corresponding to additional Λ -dependent external magnetic field χ^Λ , which is switched off in the end of the flow, if we set $\chi^{\Lambda \rightarrow 0} = 0$. In this study, we use two different counterterms with linear and exponential cutoff dependence

$$\begin{aligned} \chi_1^\Lambda &= \tilde{H} \min(1, \Lambda/\Lambda_c), \\ \chi_2^\Lambda &= \frac{\tilde{H}}{1 + \exp[(\Lambda_c - \Lambda)/\Lambda_0]}, \end{aligned} \quad (3)$$

that allow to begin the fRG flow with state at the field $H_{\text{ini}} = H + \chi^{\Lambda \rightarrow \infty} = H + \tilde{H}$, while at the end of the fRG flow one obtains renormalized vertices describing the system in the physical field $H_{\text{fin}} = H$; Λ_c , \tilde{H} and Λ_0 are independent parameters, $\Lambda_c \gg \Lambda_0$.

One can see from Fig. 1 that use of the counterterm technique eliminates the unphysical behaviour of the conductance at low magnetic fields. In the presence of counterterm, $\Sigma_\sigma^{\Lambda \rightarrow 0}$ converges to a finite value [35], which entails the nonzero value of the conductance and significantly improves agreement with the NRG data. Although the calculated conductance deviates slightly from the corresponding NRG results, the conductance per spin almost reaches the unitary limit value at zero magnetic field, $G_\sigma(H=0)|_{V_g=0} \approx 0.98e^2/h$.

We have verified that the proposed fRG scheme is stable with respect to a choice of the actual form of the counterterm, as well as parameters Λ_c , \tilde{H} , and Λ_0 . In particular, in Fig. 2 we plot the dependence of the effective energy levels of the quantum dots $\epsilon_{j,\sigma}^\Lambda = \epsilon_\sigma^0 + \Sigma_{jj,\sigma}^\Lambda$

on the cutoff parameter Λ in different schemes. One can see, that although the flow of the levels is scheme dependent, the final result does not depend on the scheme and initial magnetic field; the latter can be varied in a rather broad range.

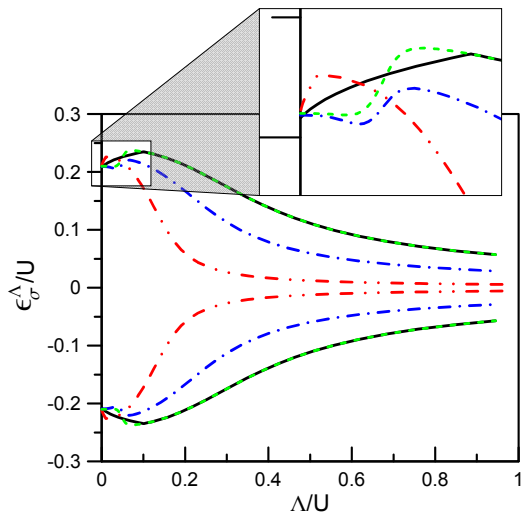


FIG. 2. (Color online). Renormalization of the energy levels $\epsilon_\sigma^\Lambda = \epsilon_{1(2),\sigma}^\Lambda$ in the fRG approximation with different counterterms for $U = 2\Gamma$ and $H = V_g = 0$. Solid (black) line and dashed-dotted-dotted (red) lines: the linear counterterm ($\tilde{H}/\Lambda_c = 2$) with $\tilde{H} = 0.2$ and $\tilde{H} = 0.02$, respectively. Dashed (green) and dashed-dotted (blue) lines: exponential counterterm ($\Lambda_c = 0.05, \Lambda_0 = 0.005$) with $\tilde{H} = 0.2$ and $\tilde{H} = 0.1$, respectively.

Spin splitting and local moments in the SFL phase.

From Fig. 2 one can see, that the spin splitting of electronic states in the end of the flow remains finite even when $H \rightarrow 0$. As we discuss below, this splitting holds in some region $|V_g| < V_g^c$ near the half-filling and reflects the formation of local moment in this range of gate voltages. The local moment appears due to the specific charge redistribution between the even and odd orbitals $d_{e(o),\sigma} = (d_{1,\sigma} \pm d_{2,\sigma})/\sqrt{2}$, which yields one electron in the odd orbital, disconnected from leads, and change the character of the spin-spin correlations [14, 35]. To show this explicitly, we plot the total occupation numbers $\langle n_{e(o)} \rangle = \sum_\sigma \langle n_{e(o),\sigma} \rangle = \sum_\sigma \langle d_{e(o),\sigma}^\dagger d_{e(o),\sigma} \rangle$ in Fig. 3(a). In agreement with Ref. [14] in finite range of gate voltages $|V_g| < V_g^c$ the odd orbital is occupied by one electron $\langle n_o \rangle = 1$, forming a $S = 1/2$ local moment, which is aligned along the direction of the magnetic field. The occupation numbers $\langle n_{e,\sigma} \rangle$ for the even orbital behave smoothly due to the level broadening caused by the hybridization of the even orbital with leads. In Fig. 3(b) we also plot the gate voltage dependence of the square of the spin in the even(odd) orbitals $\langle \mathbf{S}_{e(o)}^2 \rangle = (1/4) \sum_{\sigma,\sigma'} \langle (d_{e(o),\sigma}^\dagger \boldsymbol{\sigma} d_{e(o),\sigma'})^2 \rangle$ ($\boldsymbol{\sigma}$ are the Pauli matrices). The square of the spin on the odd orbital, $\langle \mathbf{S}_o^2 \rangle$ is equal to $S(S+1) = 3/4$ in the region

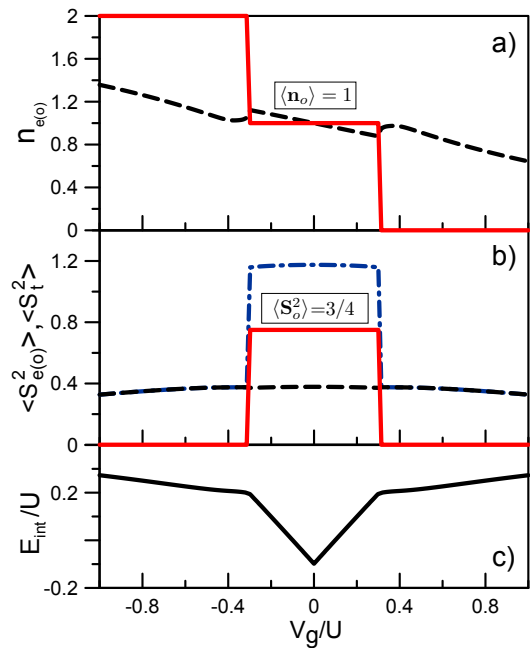


FIG. 3. (Color online). a) and b) The occupation numbers $\langle n_{e(o)} \rangle$ and the average square of magnetic moment $\langle \mathbf{S}_{e(o)}^2 \rangle$ in the even (dashed (black) lines) and odd (solid (red) lines) orbitals, as well as the average of the square of the total spin $\langle \mathbf{S}_t^2 \rangle = \langle (\mathbf{S}_1 + \mathbf{S}_2)^2 \rangle$ (dashed-dotted (blue) line) as a function of the gate voltage; (c) The interaction energy E_{int} of the double quantum dot system as a function of V_g/U .

$|V_g| < V_g^c$ and becomes zero for the $|V_g| > V_g^c$. In contrast, the square of the spin in the even orbital behaves smoothly and does not shows a significant change at the $V_g = \pm V_g^c$.

The dependence of the interaction energy $E_{\text{int}} = E - E_0$, i.e. a difference between the energy E of interacting and E_0 of non-interacting systems, on the gate voltage (shown in Fig. 3(c)) indicates that the jumps of occupation numbers correspond to the cusp of the $E(V_g)$ dependence, confirming first-order phase transition at $|V_g| = V_g^c$.

In order to understand the mechanism that leads to the existence of spin splitting of energy levels in the SFL state, we rewrite the Hamiltonian (1) in terms of even and odd orbitals (up to a constant contribution) as

$$\mathcal{H}_{\text{dot}} = \sum_{k,\sigma} \left(\epsilon_\sigma^0 - \frac{U}{2} \right) n_{k,\sigma} - U \vec{\mathbf{S}}_e \vec{\mathbf{S}}_o + \frac{U}{2} \left[n_{e,\uparrow} n_{e,\downarrow} + n_{o,\uparrow} n_{o,\downarrow} + \frac{1}{2} n_o n_e + \left(d_{e,\uparrow}^\dagger d_{o,\uparrow} d_{e,\downarrow}^\dagger d_{o,\downarrow} + \text{H.c.} \right) \right]. \quad (4)$$

The Hamiltonian (4) has a form of the two-orbital Anderson model with intra-orbital, inter-orbital, Hund exchange interaction, and pair electron hopping equal to $U/2$. In the SFL (local moment) phase even for the infinitesimally small magnetic field, the Hund exchange

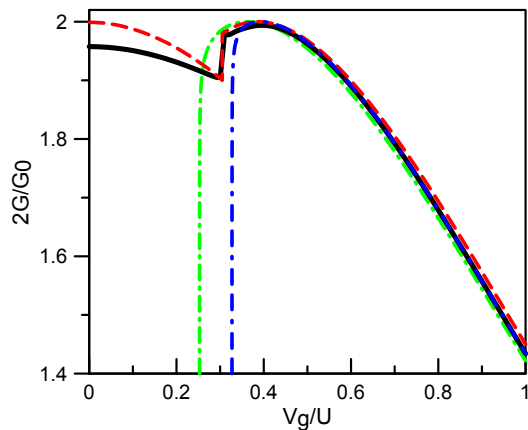


FIG. 4. (Color online). The dependence of linear conductance G on gate voltage V_g for $U = 2\Gamma$ and $H \rightarrow 0$ (at temperature $T = 0$). Solid black line: fRG approach with the linear counterterm ($\tilde{H} = 0.1, \Lambda_c = 0.05$). Dashed red line: NRG calculation. Dashed-dotted green and dashed-dashed dotted blue lines are fRG approaches in the sharp-cutoff and Litim-type cutoff scheme without counterterm.

leads to strong splitting of itinerant electronic states

$$-U\vec{S}_e\vec{S}_o \sim -\frac{U}{4} \sum_{\sigma} \sigma n_{e,\sigma}.$$

As a result the Zeeman energy splitting of even states becomes $\Delta_{\uparrow\downarrow} \sim U/2$, instead of $\Delta_{\uparrow\downarrow} = H$ in the absence of interaction U , and therefore it is strongly enhanced. Due to half filling of the odd orbital, the pair hopping term is not active in the SFL phase.

The results showing spin splitting in SFL phase refer to $H \rightarrow 0$ limit of Green functions at $T = 0$. Presence of the local moment makes however non-commutative limits $T \rightarrow 0$ and $H \rightarrow 0$. In the opposite limit $H = 0, T \rightarrow 0$ our NRG calculations confirm the validity of Logan et al. result [41], expressing the Green function through the arithmetic average of spin-split Green functions $\mathcal{G}(H = 0) = (\mathcal{G}_{\uparrow} + \mathcal{G}_{\downarrow})/2$, calculated at small finite magnetic field (which can be therefore extracted from fRG calculation).

Conductance. The resulting dependence of the conductance $G(V_g)$, obtained at $T = 0$ and $H \rightarrow 0$ according to the standard Landauer approach [35] is represented in Fig. 4. We can see that while the conductance within the both sharp and smooth cutoffs drops to zero in the SFL state, the fRG approach with the cutoff procedure (2) leads to a finite conductance in the whole range $|V_g| < V_g^c$, which agrees well with NRG results. The conductance in fRG almost reaches unitary value $G_0 = 2e^2/h$ at $V_g = 0$ and shows discontinuity at the gate voltage V_g^c , corresponding to a quantum phase transition from SFL to a regular FL ground state, in agreement with previous NRG analysis [13] for strong on-site Coulomb repulsion. The conductance in the opposite limit $T \rightarrow 0$ at $H = 0$ may differ from the above result due to additional phase shift [41]. Neglecting vertex corrections, the conductance in this limit is given by $G_0\Gamma^2 |\sum_{i,j} \mathcal{G}_{ij}(H = 0)|^2$, which yields somewhat smaller value, than at $T = 0, H \rightarrow 0$.

Conclusion. In summary, we have proposed the version of the functional renormalization-group approach, which is able to describe interaction-induced local moments in quantum dot systems, which occur due to peculiarities of geometric structure of these systems. We applied the proposed scheme to obtain occupation numbers, square of the spin, and conductance as a function of gate voltage in parallel quantum dots, symmetrically coupled to leads, and found good agreement with NRG calculations. Investigation of the gate voltage dependence of the interaction energy shows confirms first order quantum phase transition at the gate voltage V_g^c where abovementioned quantities show a jump.

The proposed approach can be further used for describing equilibrium and non-equilibrium processes in complex quantum dot systems or organic molecules. The presence of local moments in some geometries of these systems can be in particular utilized in quantum computation devices.

Acknowledgements. The work is performed within the theme Electron 01201463326 of FASO, Russian Federation, and partially supported within the Act 211 Government of the Russian Federation, contract 02.A03.21.0006. Calculations were performed on the Uran cluster of Ural branch RAS.

-
- [1] L. P. Kouwenhoven, C. M. Marcus, P. L. McEuen, S. Tarucha, R. M. Westervelt and N. S. Wingreen in *Mesoscopic Electron Transport*, NATO ASI Series E vol. **345**, edited by L. L. Sohn, L. P. Kouwenhoven, and G. Schön (Kluwer Academic Publishers, Dordrecht/Boston/London, 1997), p. 105.
- [2] J. F. Song, Y. Ochiai, and J. P. Bird, *Appl. Phys. Lett.* **82**, 4561 (2003).
- [3] D. D. Awschalom, N. Samarth, and D. Loss, eds., *Semiconductor Spintronics and Quantum Computation*, Springer (Heidelberg, 2002).
- [4] C. H. Bennett and D. P. DiVincenzo, *Nature* **404**, 247 (2000).
- [5] D. Loss and D. P. DiVincenzo, *Phys. Rev. A* **57**, 120 (1998).
- [6] H. A. Engel, L. P. Kouwenhoven, D. Loss, and C. M. Marcus, *Quantum Information Processing* **3**, 115 (2004).
- [7] R. Hanson, L. P. Kouwenhoven, J. R. Petta, S. Tarucha, L. M. K. Vandersypen, *Rev. Mod. Phys.* **79**, 1217 (2007).
- [8] J. R. Petta, A. C. Johnson, J. M. Taylor, E. A. Laird, A. Yacoby, M. D. Lukin, C. M. Markus, M. P. Hanson, and A. C. Gossard, *Science* **309**, 2180 (2005).
- [9] A. C. Hewson *The Kondo problem to Heavy Fermions*, Cambridge University Press (Cambridge, 1997).

- [10] D. Goldhaber-Gordon, H. Shtrikman, D. Mahalu, D. Abusch-Magder, U. Meirav, and M. A. Kastner, *Nature* **391**, 156 (1998).
- [11] S. M. Cronenwett, T. H. Oosterkamp, and L. P. Kouwenhoven, *Science* **281**, 540 (1998).
- [12] W. G. van der Wiel, S. De Franceschi, T. Fujisawa, J. M. Elzerman, S. Tarucha, and L. P. Kouwenhoven, *Science*, **289**, 2105, (2000).
- [13] R. Žitko and J. Bonča, *Phys. Rev. B* **76**, 241305(R) (2007).
- [14] R. Žitko, J. Mravlje, and K. Haule, *Phys. Rev. Lett.* **108**, 066602 (2012).
- [15] A. Oguri and A. C. Hewson, *J. Phys. Soc. Jpn.* **74**, 988 (2005).
- [16] Y. Nisikawa and A. Oguri, *Phys. Rev. B* **73**, 125108 (2006).
- [17] T. Numata, Y. Nisikawa, A. Oguri, and A. C. Hewson, *Phys. Rev. B* **80**, 155330 (2009).
- [18] R. López, T. Rejec, J. Martinek, and R. Žitko, *Phys. Rev. B* **87**, 035135 (2013).
- [19] A. Valli, G. Sangiovanni, O. Gunnarsson, A. Toschi, K. Held, *Phys. Rev. Lett.* **104**, 246402 (2010).
- [20] A. Valli, T. Schfer, P. Thunstrm, G. Rohringer, S. Andergassen, G. Sangiovanni, K. Held, A. Toschi, *Phys. Rev. B* **91**, 115115 (2015).
- [21] S. Florens, *Phys. Rev. Lett.* **99**, 046402 (2007).
- [22] D. Jacob, K. Haule, and G. Kotliar, *Phys. Rev. B* **82**, 195115 (2010).
- [23] V. Turkowski, A. Kabir, N. Nayyar, and T. S. Rahman, *J. Chem. Phys.* **136**, 114108 (2012).
- [24] A. Valli, G. Sangiovanni, A. Toschi, K. Held, *Phys. Rev. B* **86**, 115418 (2012).
- [25] A. K. Mitchell and R. Bulla, *Phys. Rev. B* **92**, 155101 (2015).
- [26] C. Wetterich, *Phys. Lett. B* **301**, 90 (1993).
- [27] M. Salmhofer and C. Honerkamp, *Prog. Theor. Phys.* **105**, 1 (2001).
- [28] W. Metzner, M. Salmhofer, C. Honerkamp, V. Meden, and K. Schönhammer, *Rev. Mod. Phys.* **84**, 299 (2012).
- [29] S. Andergassen, T. Enss, and V. Meden, *Phys. Rev. B* **73**, 153308 (2006).
- [30] C. Karrasch, T. Enss, and V. Meden, *Phys. Rev. B* **73**, 235337 (2006).
- [31] V. Meden in *Advances in Solid State Physics* vol. **46**, edited by R. Haug, Springer (Berlin, Heidelberg, 2008), p. 183.
- [32] V. Meden and F. Marquardt, *Phys. Rev. Lett.* **96**, 146801 (2006).
- [33] R. Gersch, J. Reiss, and C. Honerkamp, *New J. Phys.* **8**, 320 (2006).
- [34] R. Gersch, C. Honerkamp, and W. Metzner, *New J. Phys.* **10**, 045003 (2008).
- [35] See Supplementary Material for the explicit form of the Hamiltonian, fRG equations, spin dependent occupation numbers, and the conductance.
- [36] R. Bulla, T. Costi, and T. Pruschke, *Rev. Mod. Phys.* **80**, 395 (2008).
- [37] For our NRG calculations we used the open-access Budapest NRG code, developed by O. Legeza, C. P. Moca, A. I. Tóth, I. Weymann, G. Zaránd, arXiv:0809.3143 (<http://neumann.phy.bme.hu/~dmnrg/>). For details see also: A. I. Toth, C. P. Moca, O. Legeza, and G. Zarand, *Phys. Rev. B* **78**, 245109 (2008).
- [38] To calculate the conductance within NRG we consider phase shifts, see, e.g. A. Oguri, Y. Nisikawa, and A. C. Hewson, *J. Phys. Soc. Jpn.* **74**, 2554 (2005).
- [39] D. F. Litim, *Phys. Rev. D* **64**, 105007 (2001).
- [40] V. S. Protsenko and A. A. Katanin, *J. Phys.: Conf. Ser.* **690**, 012028 (2016).
- [41] D. E. Logan, A. P. Trucker, and M. R. Galpin, *Phys. Rev. B* **90**, 075150 (2014).

**SUPPLEMENTARY MATERIAL FOR THE
PAPER "INTERACTION INDUCED LOCAL
MOMENTS IN PARALLEL QUANTUM DOTS"**

V. S. Protsenko and A. A. Katanin

**A. The Hamiltonian and the noninteracting dot
Green function $\mathcal{G}_0(i\omega)$**

The Hamiltonian considered in the main text is given by $\mathcal{H} = \mathcal{H}_{\text{dot}} + \mathcal{H}_{\text{leads}} + \mathcal{H}_{\text{coupl}}$, where the quantum dots part \mathcal{H}_{dot} is described by Eq. (1) of the main text. The leads are modeled by the tight-binding Hamiltonian

$$\mathcal{H}_{\text{lead}} = -\tau \sum_{\alpha=L,R} \sum_{j=0}^{\infty} \sum_{\sigma} (c_{\alpha,j+1,\sigma}^{\dagger} c_{\alpha,j,\sigma} + \text{H.c.}). \quad (\text{S1})$$

Here $c_{\alpha,j,\sigma}^{\dagger}$ ($c_{\alpha,j,\sigma}$) are the leads creation (annihilation) operators for an electron with spin direction σ on the j lattice site of the left $\alpha = L$ or right $\alpha = R$ lead and τ is the hopping matrix element in the leads. The coupling between dots and leads are described by

$$\mathcal{H}_{\text{coupl}} = -t \sum_{\alpha=L,R} \sum_{j,\sigma} (c_{\alpha,0,\sigma}^{\dagger} d_{j,\sigma} + \text{H.c.}), \quad (\text{S2})$$

where t is the corresponding hopping. After the canonical transformation to the even $d_{e,\sigma}$ and the odd $d_{o,\sigma}$ orbitals

$$d_{e(o),\sigma} = (d_{1,\sigma} \pm d_{2,\sigma})/\sqrt{2} \quad (\text{S3})$$

the coupling part $\mathcal{H}_{\text{coupl}}$ takes the form

$$\mathcal{H}_{\text{coupl}} = -\tilde{t} \sum_{\alpha=L,R} \sum_{\sigma} (c_{\alpha,0,\sigma}^{\dagger} d_{e,\sigma} + \text{H.c.}) \quad (\text{S4})$$

with $\tilde{t} = \sqrt{2}t$. Therefore, only the even orbital is directly connected to the leads.

After projection of the leads and taking the wide-band limit $\tau \rightarrow \infty$ (keeping $t \propto \tau^{1/2}$, see Ref. [30] of the paper and [S1, S2] of this material), the inverse of the noninteracting propagator reads as

$$\mathcal{G}_{0,\sigma}^{-1}(i\omega) = (i\omega - \epsilon_{\sigma}^0) I + i\Gamma E \text{sign}(\omega) \quad (\text{S5})$$

with the energy independent hybridization strength $\Gamma = \pi|t|^2 \rho_{\text{lead}}(0)$, where ρ_{lead} is the local density of states at the last site of the left or right lead (the leads are equivalent). The I and E denote the identity and all-ones 2×2 matrices, respectively, and ϵ_{σ}^0 are the one-particle energy levels (see main text).

B. The fRG equations

Truncating the fRG flow equations by neglecting frequency dependence of the self-energy and two-particle

vertices, and the flow of the three-particle vertex functions, we obtain the closed system of the fRG flow equations for the self-energy (one-particle vertex) Σ^{Λ} ,

$$\partial_{\Lambda} \Sigma_{\alpha'}^{\Lambda}{}_{\alpha} = - \int \frac{d\omega}{2\pi} e^{i\omega 0^+} \mathcal{S}_{\beta\beta'}^{\Lambda}(i\omega) \Gamma_{\alpha'\beta'\alpha\beta}^{\Lambda}, \quad (\text{S6})$$

and for the effective two-particle interactions (two-particle vertex) Γ^{Λ} ,

$$\begin{aligned} \partial_{\Lambda} \Gamma_{\alpha'\beta'\alpha\beta}^{\Lambda} &= \int \frac{d\omega}{2\pi} \mathcal{S}_{\gamma\gamma'}^{\Lambda}(i\omega) \mathcal{G}_{\delta\delta'}^{\Lambda}(-i\omega) \Gamma_{\alpha'\beta'\delta'\gamma'}^{\Lambda} \Gamma_{\delta'\gamma'\alpha\beta}^{\Lambda} \\ &- \int \frac{d\omega}{2\pi} \mathcal{S}_{\gamma\gamma'}^{\Lambda}(i\omega) \mathcal{G}_{\delta\delta'}^{\Lambda}(i\omega) \\ &\times \left\{ \left[\Gamma_{\alpha'\gamma'\alpha\delta}^{\Lambda} \Gamma_{\delta'\beta'\gamma\beta}^{\Lambda} + (\delta \rightleftharpoons \gamma, \delta' \rightleftharpoons \gamma') \right] \right. \\ &\left. - \left[\Gamma_{\beta'\gamma'\alpha\delta}^{\Lambda} \Gamma_{\delta'\alpha'\gamma\beta}^{\Lambda} + (\delta \rightleftharpoons \gamma, \delta' \rightleftharpoons \gamma') \right] \right\}, \end{aligned} \quad (\text{S7})$$

where the Greek multi-indices collect the dot and spin indexes and repeated indices imply summation. The \mathcal{S}^{Λ} denotes the single-scale propagator

$$\mathcal{S}^{\Lambda} = \mathcal{G}^{\Lambda} \partial_{\Lambda} (\mathcal{G}_0^{\Lambda})^{-1} \mathcal{G}^{\Lambda}, \quad (\text{S8})$$

$\mathcal{G}^{\Lambda}(i\omega) = [\mathcal{G}_0^{-1}(i\omega) - \Sigma^{\Lambda}]^{-1}$. Using the explicit form of the cutoff dependent noninteracting Green function (see Eq. (2) in the main text and Eq. (S5) in this material), the single-scale propagator can be written as

$$\begin{aligned} \mathcal{S}_{\sigma}^{\Lambda}(i\omega) &= \tilde{\mathcal{S}}_{\sigma}^{\Lambda}(i\omega) + \mathcal{S}_{\sigma}^{\times}(i\omega) = i\Theta(\Lambda - |\omega|) \text{sign}(\omega) \\ &\times \left[\mathcal{G}_{\sigma}^{\Lambda}(i\omega) \right]^2 + \sigma \frac{\dot{\chi}^{\Lambda}}{2} \left[\mathcal{G}_{\sigma}^{\Lambda}(i\omega) \right]^2. \end{aligned} \quad (\text{S9})$$

The integrals, appearing at the r.h.s of the fRG equations and containing $\tilde{\mathcal{S}}_{\sigma}^{\Lambda}(i\omega)$ are analytically computed:

$$\int \frac{d\omega}{2\pi} \tilde{\mathcal{S}}^{\Lambda}(i\omega) = \frac{i\Lambda}{2\pi} \left([\mathcal{G}_+^{\Lambda}]^2 - [\mathcal{G}_-^{\Lambda}]^2 \right), \quad (\text{S10})$$

and

$$\begin{aligned} \int \frac{d\omega}{2\pi} \tilde{\mathcal{S}}_{\gamma,\gamma'}^{\Lambda}(i\omega) \mathcal{G}_{\delta,\delta'}^{\Lambda}(\mp i\omega) &= \\ \frac{i\Lambda}{2\pi} \left([\mathcal{G}_+^{\Lambda}]_{\gamma,\gamma'}^2 [\mathcal{G}_{\mp}^{\Lambda}]_{\delta,\delta'} - [\mathcal{G}_-^{\Lambda}]_{\gamma,\gamma'}^2 [\mathcal{G}_{\pm}^{\Lambda}]_{\delta,\delta'} \right), \end{aligned} \quad (\text{S11})$$

where $\mathcal{G}_{\pm}^{\Lambda} = \mathcal{G}^{\Lambda}(\pm i\Lambda)$.

Finally, the interacting part of the energy energy can be obtained from the flow equation (see Ref. [28] of the paper and [S1] of this material)

$$\partial_{\Lambda} E_{\text{int}}^{\Lambda} = \int \frac{d\omega}{2\pi} e^{i\omega 0^+} \sum_{\alpha} \left[(\mathcal{G}_0^{\Lambda} - \mathcal{G}^{\Lambda}) \partial_{\Lambda} [\mathcal{G}_0^{\Lambda}]^{-1} \right]_{\alpha\alpha}. \quad (\text{S12})$$

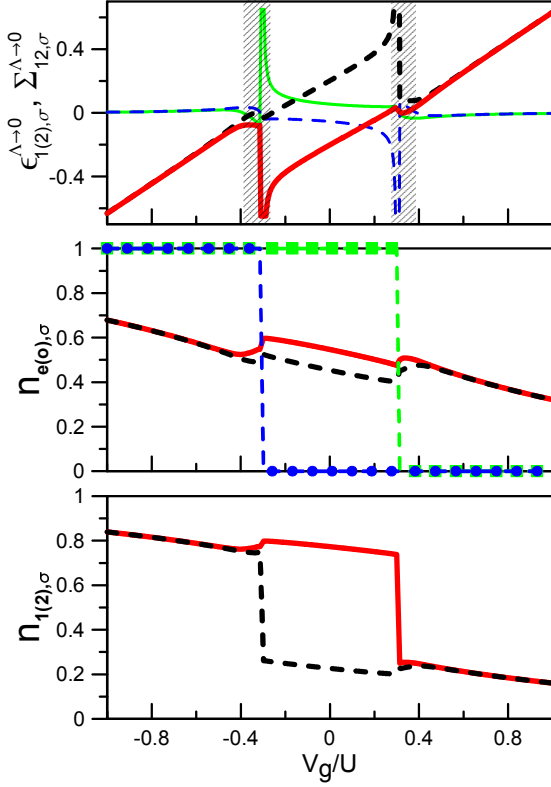


FIG. S1. The spin-resolved results of fRG with the counterterm for $U = 2\Gamma$. Upper panel: Effective energy levels $\epsilon_{1(2),\sigma}^{\Lambda \rightarrow 0}$ (thick solid (red) and dashed (black) line for $\sigma = \uparrow, \downarrow$, respectively) and off-diagonal self-energies (effective hopping between the levels) $\Sigma_{12,\sigma}^{\Lambda \rightarrow 0}$ (thin solid (green) and dashed (blue) line for $\sigma = \uparrow, \downarrow$) in units of U as a function of the gate voltage. Middle panel: the average occupation numbers in the even $\langle n_{e,\sigma} \rangle$ (solid (red) line and dashed (black) line for $\sigma = \uparrow, \downarrow$) and odd $\langle n_{o,\sigma} \rangle$ (green squares and blue circles for $\sigma = \uparrow, \downarrow$) energy levels as a function of the gate voltage. Bottom panel: the average occupation numbers $\langle n_{1(2),\sigma} \rangle$ (solid (red) line and dashed (black) line for $\sigma = \uparrow, \downarrow$) as a function of the gate voltage. All calculations were performed for $H = 0$ within the fRG approach with the linear counterterm ($\tilde{H} = 0.1, \Lambda_c = 0.05$).

C. Self-energies and occupation numbers

From the self-energies, obtained in fRG procedure, occupation numbers at zero temperature are given by the standard expression

$$\langle n_{j,\sigma} \rangle = \int \frac{d\omega}{2\pi} e^{i\omega 0^+} \left[[\mathcal{G}_{0,\sigma}^{\Lambda=0}(i\omega)]^{-1} - \Sigma_{\sigma}^{\Lambda \rightarrow 0} \right]_{jj}^{-1}. \quad (\text{S13})$$

Using the explicit form of the bare Green function $\mathcal{G}_{0,\sigma}(i\omega)$ (see Eq. (S5) in this supplement), one can obtain

$$\langle n_{\sigma} \rangle = \frac{1}{2} - \frac{1}{2\pi} \arctan\left(\frac{\epsilon_{e,\sigma}}{2\Gamma}\right) - \frac{1}{4} \text{sign}(\epsilon_{o,\sigma}), \quad (\text{S14})$$

where $\langle n_{\sigma} \rangle = \langle n_{1(2),\sigma} \rangle$ and $\epsilon_{e(o),\sigma} = (\epsilon_{\sigma}^o + \Sigma_{11}^{\sigma}) \pm \Sigma_{12}^{\sigma}$ are the on-site energies of the even and odd orbitals. Eq. (S14) can be clearly interpreted in terms of the occupancies of the even/odd states. Indeed, after the transformation (S3) we obtain the even states with energies $\epsilon_{e,\sigma}$ and hybridization $\Gamma_e = 2\Gamma$, and therefore $\langle n_{e,\sigma} \rangle = 1/2 - \frac{1}{\pi} \arctan\left(\frac{\epsilon_{e,\sigma}}{2\Gamma}\right)$, as well as the odd states $\epsilon_{o,\sigma}$, which are non-hybridized with the leads $\Gamma_o = 0$, hence $\langle n_{o,\sigma} \rangle = \frac{1}{2} (1 - \text{sign}(\epsilon_{o,\sigma}))$. Thus, using that

$$\langle n_{\sigma} \rangle = \frac{1}{2} \sum_j \langle n_{j,\sigma} \rangle = \frac{1}{2} (\langle n_{e,\sigma} \rangle + \langle n_{o,\sigma} \rangle), \quad (\text{S15})$$

we again obtain Eq. (S14).

The results of the calculation of spin-dependent self-energies and occupation numbers are shown in Fig. S1. One can see that the self-energies and occupation numbers are strongly split (with respect to spin projection) at $|V_g| < V_c$. There is small splitting of self-energies also in the vicinity of the transition point in the paramagnetic phase (in the shaded area), which is an artifact of the present approach. We also note, that in the vicinity of the transition point, the proposed fRG approach may overestimate the renormalization of the vertices and for this reason may become less accurate for $V_g \approx V_g^c$ (in the shaded areas in the Fig. S1a). However, we have found that even for these gate voltages all the observables are described correctly in comparison with the NRG calculations.

D. The linear conductance

If the full Green function $\mathcal{G}_{\sigma}(i\omega)$ is known, the linear conductance of an interacting system at zero temperature can be computed as (see, e.g., Ref. [30] of the paper)

$$G = G_0 \frac{\Gamma^2}{2} \sum_{\sigma} \left| \sum_{j,j'} \mathcal{G}_{\sigma;j,j'}(0) \right|^2 = \frac{e^2}{h} \sum_{\sigma} \frac{\Gamma_e^2}{(\epsilon_{e,\sigma})^2 + \Gamma_e^2},$$

where $G_0 = \frac{2e^2}{h}$ is the conductance quantum. Taking into account Eq. (S14) the above expression for the conductance can be equivalently represented as

$$G = \frac{e^2}{h} \sum_{\sigma} \sin^2 \delta_{\sigma}^e, \quad (\text{S16})$$

where $\delta_{\sigma}^e = \pi \langle n_{e,\sigma} \rangle$.

-
- [S1] C. Karrasch, *The Functional Renormalization Group for Zero-Dimensional Quantum Systems in and out of Equilibrium*, Ph.D. thesis, RWTH Aachen, (2010); arXiv:1009.3852.
- [S2] T. Enss, *Renormalization, Conservation Laws and Transport in Correlated Electron Systems*, Ph.D. thesis, University of Stuttgart (2005); cond-mat/0504703.